Constraints on spin-independent nucleus scattering with sub-GeV WIMP dark matter from the CDEX-1B Experiment at CJPL

Z. Z. Liu,[1] Q. Yue,[1,*] L. T. Yang,[1,†] K. J. Kang,[1] Y. J. Li,[1] H. T. Wong,[3,‡] M. Agartioglu,[3,4,‡] H. P. An,[1,5] J. P. Chang,[6] J. H. Chen,[3,‡] Y. H. Chen,[7] J. P. Cheng,[1,2] Z. Deng,[1] Q. Du,[8] H. Gong,[1] X. Y. Guo,[7] L. He,[6] S. M. He,[7] J. W. Hu,[1] Q. D. Hu,[1] H. X. Huang,[9] L. P. Jia,[1] H. Jiang,[1] H. B. Li,[3,‡] H. Li,[6] J. M. Li,[1] J. Li,[1] X. Li,[9] X. Q. Li,[10] Y. L. Li,[1] B. Liao,[2] F. K. Lin,[3,‡] S. T. Lin,[8] S. K. Liu,[8] Y. D. Liu,[2] Y. Y. Liu,[2] H. Ma,[1,§] J. L. Ma,[1,5] J. H. Ning,[7] H. Pan,[6] N. C. Qi,[7] J. Ren,[9] X. C. Ruan,[9,4] V. Sharma,[3,11,‡] Z. She,[1] L. Singh,[3,11,‡] M. K. Singh,[3,11,‡] T. X. Sun,[2] C. J. Tang,[8] W. Y. Tang,[1] Y. Tian,[1] G. F. Wang,[2] L. Wang,[12] Q. Wang,[1,5] Y. Wang,[1,5] S. Y. Wu,[7] Y. C. Wu,[1] H. Y. Xing,[8] Y. Xu,[10] T. Xue,[1,5] N. Yi,[1] C. X. Yu,[10] H. J. Yu,[6] J. F. Yue,[7] M. Zeng,[1] Z. Zeng,[1] F. S. Zhang,[2] M. G. Zhao,[10] J. F. Zhou,[7] Z. Y. Zhou,[9] and J. J. Zhu[8]

(CDEX Collaboration)

[1] *Key Laboratory of Particle and Radiation Imaging (Ministry of Education) and Department of Engineering Physics, Tsinghua University, Beijing 100084*
[2] *College of Nuclear Science and Technology, Beijing Normal University, Beijing 100875*
[3] *Institute of Physics, Academia Sinica, Taipei 11529*
[4] *Department of Physics, Dokuz Eylül University, İzmir 35160*
[5] *Department of Physics, Tsinghua University, Beijing 100084*
[6] *NUCTECH Company, Beijing 100084*
[7] *YaLong River Hydropower Development Company, Chengdu 610051*
[8] *College of Physical Science and Technology, Sichuan University, Chengdu 610065*
[9] *Department of Nuclear Physics, China Institute of Atomic Energy, Beijing 102413*
[10] *School of Physics, Nankai University, Tianjin 300071*
[11] *Department of Physics, Banaras Hindu University, Varanasi 221005*
[12] *Department of Physics, Beijing Normal University, Beijing 100875*

(Dated: May 2, 2019)

We report results on the searches of weakly interacting massive particles (WIMPs) with sub-GeV masses (m_χ) via WIMP-nucleus spin-independent scattering with Migdal effects and bremsstrahlung emissions incorporated. Analysis on time-integrated (TI) and annual modulation (AM) effects on CDEX-1B data are performed, with 737.1 kg·day exposure and 160 eVee threshold for TI analysis, 1107.5 kg·day exposure and 250 eVee threshold for AM analysis. The sensitive windows in m_χ are expanded by an order of magnitude. New limits on $\sigma^{\rm SI}_{\chi N}$ at 90% confidence level at $m_\chi \sim 0.05{-}0.18$ GeV/c^2 and $0.075{-}3.0$ GeV/c^2 in the TI and AM analysis are derived, respectively.

PACS numbers: 95.35.+d, 29.40.-n, 98.70.Vc

Introduction. Weakly interacting massive particles (WIMPs, denoted as χ) are the most popular candidates of dark matter, the searches of which are of intense experimental interest [1]. Direct detection experiments such as XENON [2], LUX [3], PandaX [4], CDMSlite [5], DarkSide [6], CDEX [7–12] are based on WIMP-nucleus (χ-N) elastic scatterings through spin-independent (SI) and spin-dependent (SD) interactions. However, the nuclear recoil energy and hence the experimental observable rapidly diminishes with decreasing m_χ. Detectors with low threshold have to be used to study these light WIMPs. At the lowest achieved threshold of 30.1 eV in nuclear recoil energy, the CRESST [13] experiment extends the reach of m_χ to below 0.16 GeV/c^2, using the conventional χ-N scattering detection channel.

It is recently pointed out that finite amount of electrons or photons are produced in χ-N scattering [14–17]. Two of the mechanisms that produce electro-magnetic final states in χ-N scatterings are Migdal effect [15, 16] and bremsstrahlung emissions [17]. The observable signals due to electron recoils or gamma rays are much larger than those of nuclear recoils at m_χ less than several few GeV. Taking these two effects into account, the lower reach of m_χ in direct detection experiments can be substantially extended to domains far below 1 GeV/c^2.

P-type point contact germanium (PPCGe) detectors have been adopted by CDEX [7–12] in light WIMP searches, exploiting their good energy resolution and ultra-low energy threshold. Located in the China Jinping Underground Laboratory (CJPL) [18], CDEX-1B experiment [11] has for its target a single-element PPCGe detector cooled by a cold finger, with an active mass of 939 g. A NaI(Tl) anti-Compton detector is used as active shielding. The detector has been under stable data taking conditions since March 27, 2014 and limits on χ-N SI-scattering down to $m_\chi{\sim}2$ GeV/c^2 are derived at an energy threshold of 160 eVee ("eVee" represents the electron equivalent energy) with an exposure of 737.1 kg·day [11]. In this letter, taking Migdal effect and bremsstrahlung emissions into account, the CDEX-1B data is re-analyzed to derive new limits on χ-N SI-interactions, cross-section of which denoted by $\sigma^{\rm SI}_{\chi N}$.

Migdal effect and bremsstrahlung emissions. The conventional and simplified treatment of χ-N scattering is that all the kinetic energy is transferred from χ to nuclear recoil via elastic scattering. Complexities arise in real physical systems, since the target nuclei in detectors, being part of the atoms, are coupled also to the electrons. There is finite probability that high-energy electrons are ejected via inelastic processes. The electrons do not follow the motion of the nuclei such that the ionization characteristics to the target medium from the electron recoils are different from those of nuclear recoils where the ionization energy is quenched due to recombinations. The process, called Migdal effect [19–21] were recently studied in the context of WIMP detection via χ-N interactions [15, 16]. The probability of having two or more electrons ionized or excited in an interaction is much smaller than those with only one electron. Therefore, only single electron excitation and ionization is considered. The total transition rates are the summation of ionization and excitation probabilities and the probability for the recoil atoms to remain in ground state, which is given by Eq. (4.12) in Ref. [15]. According to Ref. [15], the excitation probability is much smaller than ionization probability, especially for inner shell electron, so the excitation is also neglected.

After an electron is ejected via ionization, the ionized atom will de-excite and emit new electrons or photons, whose total energy is the binding energy, denoted as E_{nl}. The total electronic energy, distinctive from the nuclear recoil energy, is given by $E_{EM} = E_e + E_{nl}$, where E_e is the kinetic energy of electron after ionization, while the cross section is given by

$$\frac{d^2\sigma}{dE_R dE_{EM}} = \frac{d\sigma}{dE_R}\frac{1}{2\pi}\sum_{n,l}\frac{d}{dE_{EM}}p^c_{q_e}(nl \to (E_{EM} - E_{nl})), \tag{1}$$

where E_R is the nuclear recoil energy, q_e is equal to $m_e q_A/m_A$, m_A is the atomic mass approximated to target nucleus mass, and q_A is equal to $\sqrt{2m_A E_R}$, n and l are the principal quantum number and orbital quantum number, respectively.

The maximum energy of electronic energy $E_{EM,max}$ is equal to $1/2\mu_N v^2$, μ_N is the reduced mass, v is the relative velocity between χ and the target nucleus, while the maximum energy of nuclear recoil $E_{R,max}$ is equal to $2\mu_N^2 v^2/m_N$. If $m_\chi \ll m_N$, then $\mu_N \sim m_\chi$, such that $E_{EM,max} \gg E_{R,max}$. For example, while $m_\chi = 0.05$ GeV/c^2 and $m_N = 67.66$ GeV/c^2 (the nucleus mass of Ge), for v_{max}=776 km/s, the resulting $E_{EM,max} \approx 167$ eV and $E_{R,max} \approx 1$ eV.

As the nucleus acquires kinetic energy from χ-N scattering, the accompanying ejected electron will get accelerated in order to follow the nuclear recoil trajectory, resulting with a finite probability that a photon will be emitted through bremsstrahlung. According to Ref. [17], the photo-emission cross section (σ) is given by

$$\frac{d^2\sigma}{dE_\gamma dE_R} = \frac{4\alpha}{3\pi E_\gamma}\frac{E_R}{m_N c^2} \mid f(E_\gamma) \mid^2 \times \frac{d\sigma}{dE_R}\Theta(E_{\gamma,max} - E_\gamma), \tag{2}$$

where E_γ is the energy of photon, α is the fine structure constant, m_N is the mass of target nucleus, $f(E_\gamma) = f_1(E_\gamma) + if_2(E_\gamma)$ is the atomic scattering factors documented at the NIST Standard Reference Database [22], and Θ refers to the truncation function.

The χ-N event rates due to both Migdal effect and bremsstrahlung emissions can be expressed as:

$$\frac{d^2R}{dE_x dE_R} = N_T\frac{\rho_\chi}{m_\chi}\int d^3\vec{v}\, v f_v(\vec{v} + \vec{v}_E)\frac{d^2\sigma}{dE_x dE_R}, \tag{3}$$

where N_T is the number of target nuclei per unit detector, E_x refers to E_γ or E_{EM}, ρ_χ is the density of dark matter, m_χ is the mass of DM particle, $\vec{v}_E$ is Earth's velocity relative Galaxy.

As the CDEX PPCGe detectors do not discriminate nuclear recoils from electron recoils, the observable signals are the summation of nuclear recoil energy and electron recoil energy, denoted as $E_{det} = E_x + Q_{nr}E_R$, where Q_{nr} is the quenching factor [23]. In this letter, the Lindhard formula [24] is adopted for the evaluation of Q_{nr}. There is no experiment data for Q_{nr} of Ge below 0.2 keVnr, so the κ value (κ=0.22) in Lindhard formula is derived by fitting of experiment data [25–27] under 2 keVnr with a conservative uncertainty of 30% adopted as systematic error.

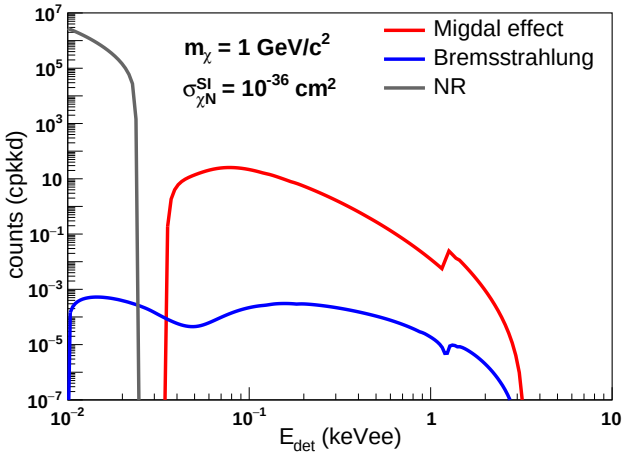

FIG. 1. Expected measureable spectra of the χ-N elastic SI-scattering (gray line), χ-N inelastic SI-scattering with Migdal effect (Red line) and bremsstrahlung emissions (blue line) incorporated. The target nucleus is Ge, the mass of WIMPs is set to 1 GeV/c^2, and $\sigma^{\rm SI}_{\chi N}$ is set to 10^{-36} cm^2. Energy resolution is not taken into account in this plot.

Time-integrated (TI) analysis. The expected energy spectrum of χ-N SI scattering is shown in Fig. 1, where

the target nucleus is Ge, $m_\chi = 1$ GeV/c^2, and $\sigma^{\rm SI}_{\chi N} = 10^{-36}$ cm^2. The standard WIMP galactic halo assumption and conventional astrophysical models [28] are used, with χ-density ρ_χ set to 0.3 GeV/(c^2 cm^3), Earth's velocity v_E at 232 km/s, χ-velocity distribution assumed to be Maxwellian with the most probable velocity $v_0 = 220$ km/s, the local Galactic escape velocity at 544 km/s, and the Helm form factor [29, 30] is adopted. Smearing due to energy resolution is taken into account in later analysis. Only the ionization spectra from L and M shell (n = 2,3) are considered, while those of K-shell are negligible, and those of the valence electrons (N shell, n=4) are not reliable.

Using Fig. 1 as illustration, the expected rates in complete energy range for χ-N elastic SI-scattering, Migdal effects and bremsstrahlung emissions at m_χ=1 GeV/c^2 are in ratio of about $8\times10^8 : 2\times10^4 : 1$. However, at a threshold of 160 eVee where the χ-N elastic scatterings are no longer observable, the Midgal effect and bremsstrahlung processes can still produce signals above threshold and therefore open the sensitivity windows to lower m_χ.

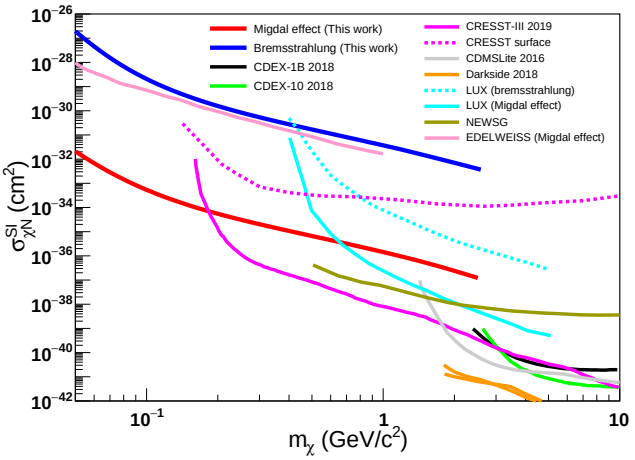

FIG. 2. Upper limits at 90% C.L on $\sigma^{\rm SI}_{\chi N}$ derived by Binned Poisson method in TI analysis using the CDEX-1B experiment data, with several benchmark experiments [5, 6, 11–13, 31–34] superimposed. Limits from nuclear recoil-only analysis with the same data set is shown (cyan line) as comparison. Migdal effect (red line) provides the best sensitivities for m_χ ~0.05−0.18 GeV/c^2.

Upper limits at 90% confidence level (C.L.) in $\sigma^{\rm SI}_{\chi N}$ are derived by Binned Poisson method [35] with the CDEX-1B TI-data [11]. The exclusion curve is shown in Fig. 2, in which several other experiments are superimposed for reference. The sensitivity to $\sigma^{\rm SI}_{\chi N}$ contributed by Migdal effect dominates over that by bremsstrahlung emissions by four to five order of magnitude. New limits are achieved for $m_\chi < 0.18$ GeV/c^2, and the lower reach is extended to 0.05 GeV/c^2.

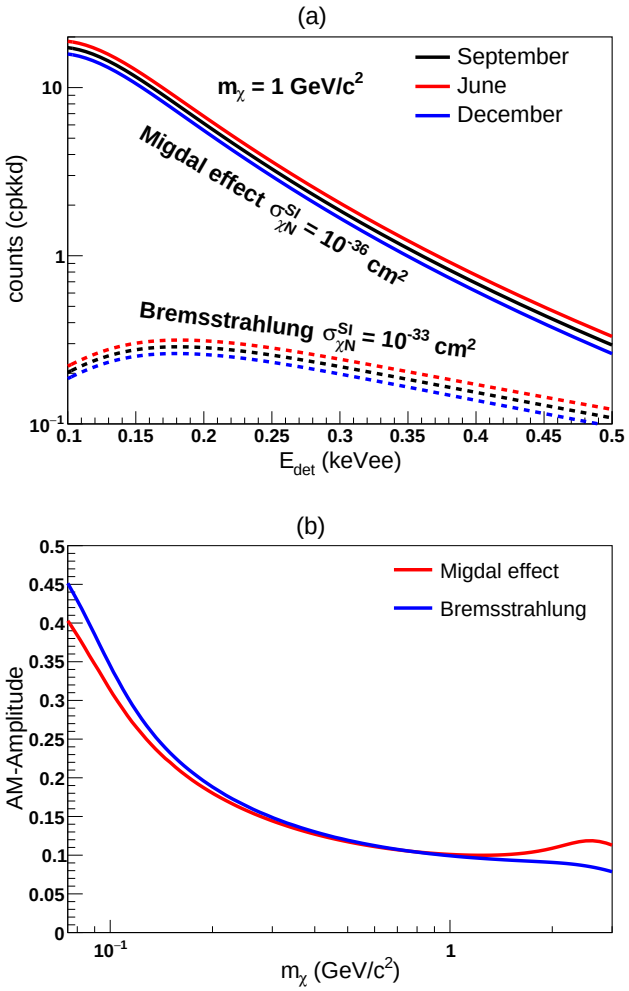

FIG. 3. (a) The solid lines are the expected spectra due Migdal effect at June (red solid line), September (black solid line) and December (blue solid line). The dashed lines are the expected spectra of bremsstrahlung emssions at June (red dashed line), September (black dashed line) and December (blue dashed line). The resolution is added on the spectra. (b) The AM-amplitude due Migdal effect (red line) and bremsstrahlung (blue line) in 0.25 − 0.3 keVee energy range at different m_χ. The AM-amplitude is defined as (R(m_χ,Jun.)-R(m_χ,Dec.))/2/R(m_χ,Sep.), where R(m_χ,t) is the expected count at the specified energy-bin, m_χ and time t.

Annual modulation (AM) analysis. Positive observations of AM would provide smoking-gun signatures for WIMPs independent of the astrophysics and background models. The Earth's velocity relative to the galactic WIMP-halo is time-varying with a period of one year, and can be expressed as $v_E = 232 + 30\times0.51\cos(2\pi/T\times(t-\Phi)$, where T is set to be 365.25 days, Φ is set to be 152.5 days from January 1st [36]. The expected measurable spectra at different time of the year are shown in Fig. 3 (a). The AM-amplitudes (summer-winter differece

in the spectra) at different m_χ are depicted in Fig. 3 (b). It can be seen that the AM-amplitudes from Migdal effect or bremsstrahlung are both enhanced at lower m_χ. Consequently, the AM analysis might provide more sensitive probes at low m_χ than TI analysis at the same energy threshold.

We adopt in this AM analysis the same data as previously used to study AM effects in the conventional χ-N nuclear recoil channel [37]. There are two datasets, Run-1 with the the NaI(Tl) anti-Compton detector, and Run-2 without NaI(Tl), having 751.3 and 428.1 live days, respectively, and together spanning a total of 1527 calendar days (∼4.2 yr) and a total exposure of 1107.5 kg·day. The background stability and environment parameters have been checked, and the time stability of the candidate χ-N event rates at different energy ranges were demonstrated with Fig. 1 of Ref. [37]. The Model-Dependent AM analysis [37] is adopted in this analysis. The AM-amplitudes (A_{ik} of the i^{th} energy-bin of the k^{th} Run) are related and constrained by a known function (f) of m_χ and $\sigma^{\rm SI}_{\chi N}$, such that $A_{ik} = \sigma^{\rm SI}_{\chi N}(m_\chi) f(E_{ik}, \delta E_{ik}; m_\chi)$, where E_{ik} and δE_{ik} are the mean energy and its corresponding bin-size, respectively. The same analysis threshold of 250 eVee and χ^2 minimization procedures are adopted [37].

Depicted in Fig. 4 are the 90% C.L. limits from AM analysis with Migdal effects and bremsstrahlung emissions. The only previous AM analysis on bremsstrahlung emissions was performed by XMASS-I [38] where threshold is higher (1 keVee). Its limits are also displayed. Superimposed for comparison are the AM nuclear recoils bounds from CDEX-1B [37] and XMASS-I [38], as well as the AM-allowed regions of CoGeNT [39, 40] and DAMA/LIBRA [21, 35, 41, 42]. The lower reach light WIMPs is extended to 0.075 GeV/c^2.

Summary. In this letter, we incorporate two newly identified mechanisms on χ-N SI-interactions to the analysis of CDEX-1B data. New m_χ windows are opened and new limits are derived. The Migdal effect has stronger impact than bremsstrahlung emissions and provides much more stringent bounds in both TI and AM analysis. The exclusion region in m_χ can be extended 0.05 GeV/c^2 with an energy threshold of 160 eVee in the TI analysis. The best sensitivity in $\sigma^{\rm SI}_{\chi N}$ is achieved for m_χ ∼(0.05−0.18) GeV/c^2 via the Migdal effect. About 4.2 years time-span of CDEX-1B data are used in the AM analysis. At an energy threshold of 250 eVee, the best sensitivity of $\sigma^{\rm SI}_{\chi N}$ for $m_\chi < 3.0$ GeV/c^2 via the Migdal effect is achieved, extending to 0.075 GeV/c^2.

This work was supported by the National Key Research and Development Program of China (Grant No. 2017YFA0402200) and the National Natural Science Foundation of China (Grants No. 11725522, No. 11675088, No.11475099).

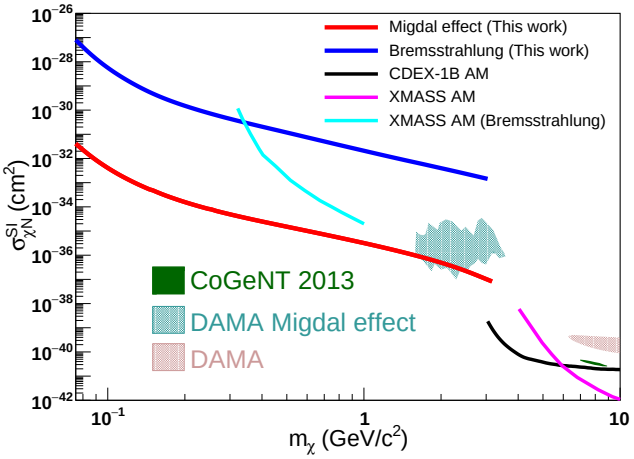

FIG. 4. Upper limit at 90% C.L. on $\sigma^{\rm SI}_{\chi N}$ derived by AM analysis using CDEX-1B data about 4.2 years [37]. The energy threshold of the modulated analysis is 250 eVee, while the reach of the exclusion line (red line and blue line) is extended to 0.075 GeV/c^2. The nuclear-recoil only limits from the same data set is superimpsed [37]. Constraints [38] and allowed regions [21, 35, 39–42] from AM analysis from other experiment are also shown.

* Corresponding author: yueq@mail.tsinghua.edu.cn
† Corresponding author: yanglt@mail.tsinghua.edu.cn
‡ Participating as a member of TEXONO Collaboration
§ Corresponding author: mahao@mail.tsinghua.edu.cn

[1] M. Tanabashi *et al.*, Phys. Rev. D **98**, 030001 (2018).
[2] E. Aprile *et al.*, Phys. Rev. Lett. **121**, 111302 (2018).
[3] D. S. Akerib *et al.*, Phys. Rev. Lett. **118**, 021303 (2017).
[4] X. Cui *et al.*, Phys. Rev. Lett. **119**, 181302 (2017).
[5] R. Agnese *et al.*, Phys. Rev. Lett. **116**, 071301 (2016).
[6] P. Agnes *et al.*, Phys. Rev. Lett. **121**, 081307 (2018).
[7] S. K. Liu *et al.*, Phys. Rev. D **90**, 032003 (2014).
[8] W. Zhao *et al.*, Phys. Rev. D **88**, 052004 (2013).
[9] Q. Yue *et al.*, Phys. Rev. D **90**, 091701 (2014).
[10] W. Zhao *et al.*, Phys. Rev. D **93**, 092003 (2016).
[11] L. T. Yang *et al.*, Chin. Phys. C **42**, 23002 (2018).
[12] H. Jiang *et al.*, Phys. Rev. Lett. **120**, 241301 (2018).
[13] A. H. Abdelhameed *et al.*, (2019), arXiv:1904.00498.
[14] C. Moustakidis, J. Vergados, and H. Ejiri, Nuc. Phys. B **727**, 406 (2005).
[15] M. Ibe, W. Nakano, Y. Shoji, and K. Suzuki, J. High Energy Phys. **03**, 194 (2018).
[16] M. J. Dolan, F. Kahlhoefer, and C. McCabe, Phys. Rev. Lett. **121**, 101801 (2018).
[17] C. Kouvaris and J. Pradler, Phys. Rev. Lett. **118**, 031803 (2017).
[18] J. P. Cheng *et al.*, Annu. Rev. Nucl. Part. Sci. **67**, 231 (2017).
[19] A. B. Migdal, J. Phys. (USSR) **4**, 449 (1941).
[20] G. Baur, F. Rosel, and D. Trautmann, J. Phys. B: At Mol. Phys. **16**, L419 (1983).
[21] R. Bernabei *et al.*, Int. J. Mod. Phys. A **22**, 3155 (2007).

[22] C. T. Chantler, J. Phys. Chem. Ref. Data **24**, 71 (1995).
[23] A. Soma *et al.*, Nucl. Instrum. Methods Phys. Res., Sect. A **836**, 67 (2016).
[24] J. Lindhard *et al.*, Mat. Fys. Medd. Dan. Vid. Selsk. **33**, 10 (1963).
[25] K. W. Jones and H. W. Kraner, Phys. Rev. C **4**, 125 (1971).
[26] K. W. Jones and H. W. Kraner, Phys. Rev. A **11**, 1347 (1975).
[27] P. S. Barbeau, J. I. Collar, and O. Tench, J. Cosmol. Astropart. Phys. **09**, 009 (2007).
[28] C. E. Aalseth *et al.*, Phys. Rev. D **88**, 012002 (2013).
[29] G. Jungman, M. Kamionkowski, and K. Griest, Phys. Rep. **267**, 195 (1996).
[30] J. Lewin and P. Smith, Astropart. Phys. **6**, 87 (1996).
[31] D. S. Akerib *et al.*, Phys. Rev. Lett. **122**, 131301 (2019).
[32] G. Angloher *et al.*, Eur. Phys. J. C **77**, 637 (2017).
[33] Q. Arnaud *et al.*, Astropart. Phys. **97**, 54 (2018).
[34] E. Armengaud *et al.*, Phys. Rev. D **99**, 082003 (2019).
[35] C. Savage *et al.*, J. of Cosmol. Astropart. Phys. **04**, 010 (2009).
[36] M. C. Smith *et al.*, Mon. Not. R. Astron. Soc. **379**, 755 (2007).
[37] L. T. Yang *et al.*, (2019), arXiv:1904.12889.
[38] M. Kobayashi *et al.*, (2019), arXiv:1808.06177.
[39] C. E. Aalseth *et al.*, Phys. Rev. D **88**, 012002 (2013).
[40] C. Aalseth *et al.*, (2014), arXiv:1401.3295.
[41] R. Bernabei *et al.*, Eur. Phys. J. C **73**, 2648 (2013).
[42] S. Baum, K. Freese, and C. Kelso, Phys. Lett. B **789**, 262 (2019).